Publishing House
AKAPIT

COMPUTER METHODS IN MATERIALS SCIENCE

Informatyka w Technologii Materiałów

Vol. 11, 2011, No. 1

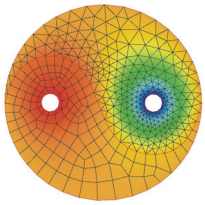

THE MLPG ANALYSIS OF CRACK PROBLEMS IN MAGNETOELECTROELASTIC SOLIDS

JAN SLADEK*, VLADIMIR SLADEK

Institute of Construction and Architecture, Slovak Academy of Sciences, 84503 Bratislava, Slovakia
**Corresponding author: jan.sladek@savba.sk*

Abstract

A meshless method based on the local Petrov-Galerkin approach is applied for boundary value problems with cracks in magnetoelectroelastic solids. A unit step function is used as the test functions in the local weak-form. This leads to local boundary-domain integral equations (LIEs). The moving least-squares (MLS) method is adopted for approximating the physical quantities in the LIEs. A system of ordinary differential equations for certain nodal unknowns is obtained. That system is solved numerically by the Houbolt finite-difference scheme. Numerical results for intensity factors in homogeneous and functionally graded materials are presented.

Key words: meshless local Petrov-Galerkin method (MLPG), moving least-squares (MLS) interpolation, intensity factors, Houbolt method, functionally graded material

1. INTRODUCTION

Piezoelectric and piezomagnetic materials offer certain potential performance advantages over conventional ones due to their capability of converting the energy from one type to other among magnetic, electric, and mechanical. Therefore, they are utilized as smart materials. Some composite materials can provide superior properties compared to their constituents. The magneto-electro-mechanical coupling in some composites can be hundred times higher than in single-phase materials (Tong et al., 2008). If the volume fraction of constituents is varying in a predominant direction, we are talking about functionally graded materials (FGMs). Originally these materials have been introduced to benefit from the ideal performance of its constituents.

The solution of general boundary value problems for continuously nonhomogeneous magneto-electroelastic solids requires advanced numerical methods due to the high mathematical complexity. Besides this complication, the magnetic, electric and mechanical fields are coupled with each other in the constitutive equations. In recent years, meshless formulations are becoming popular. The moving least squares (MLS) approximation is generally considered as one of many schemes to interpolate discrete data with a reasonable accuracy. The continuity of the MLS approximation is given by the minimum between the continuity of the basis functions and that of the weight function. In the conventional discretization methods there is a discontinuity of the secondary fields on the interface of elements. For modeling continuously nonhomogeneous solids, the approach based on piecewise continuous elements can bring some inaccuracies. Therefore, modeling based on C^1-continuity, like meshless methods, is expected to be more accurate. A variety of meshless methods has been proposed so far with some of them being applied to piezoelectric and magnetoelectroelastic problems (Liu et al., 2002; Ohs & Aluru, 2001; Sladek et al., 2007, 2008). Transient problems

 ISSN 1641-8581

are analyzed there in the Laplace transformed domain. The meshless local Petrov-Galerkin (MLPG) method is a fundamental base for the derivation of many meshless formulations, since trial and test functions can be chosen from different functional spaces. In the present paper, the MLPG method is extended to 2-D continuously nonhomogeneous magnetoelectroelastic solids with cracks. The weak-forms in the time domain for the coupled governing partial differential equations on small subdomains with a Heaviside step function as the test functions are applied to derive local integral equations. The spatial variations of the displacements, electric and magnetic potentials are approximated by the moving least-squares scheme (MLS) (Belytschko et al 1996; Atluri, 2004). After performing the spatial MLS approximation, a system of ordinary differential equations is obtained. Then, the system of the ordinary differential equations of the second order resulting from the equations of motion is solved by the Houbolt finite-difference scheme.

2. MESHLESS LOCAL INTEGRAL EQUATIONS FOR MAGNETO-ELECTRO-ELASTIC SOLIDS

The basic equations of linear magnetoelectroelastic materials consist of the governing equations (Maxwell equations and the balance of momentum) and the constitutive relations. The quasi-static Maxwell equations for the electric displacement D_j and magnetic induction B_j fields are written as

$$D_{j,j}(\mathbf{x},\tau) - R(\mathbf{x},\tau) = 0 \tag{1}$$

$$B_{j,j}(\mathbf{x},\tau) - O(\mathbf{x},\tau) = 0 \tag{2}$$

where R and O are volume density of free charges and magnetic induction source, respectively.

The remaining vector Maxwell equations in quasi-static approximation, $\nabla \times \mathbf{E} = 0$ and $\nabla \times \mathbf{H} = 0$, are satisfied, if the electric vector $\mathbf{E}(\mathbf{x},\tau)$ and magnetic intensity $\mathbf{H}(\mathbf{x},\tau)$ fields are expressed as gradients of the scalar electric and magnetic potentials $\psi(\mathbf{x},\tau)$ and $\mu(\mathbf{x},\tau)$,

$$E_j(\mathbf{x},\tau) = -\psi_{,j}(\mathbf{x},\tau) \tag{3}$$

$$H_j(\mathbf{x},\tau) = -\mu_{,j}(\mathbf{x},\tau) \tag{4}$$

To complete the set of the governing equations, eqs. (1) and (2) need to be supplemented by the balance of momentum

$$\sigma_{ij,j}(\mathbf{x},\tau) + X_i(\mathbf{x},\tau) = \rho \ddot{u}_i(\mathbf{x},\tau) \tag{5}$$

where σ_{ij}, $\ddot{u}_i$, ρ and X_i denote the stress, acceleration, the mass density, and the body force vector, respectively.

The constitutive relations represent the coupling of the mechanical and the electromagnetic fields

$$\sigma_{ij}(\mathbf{x},\tau) = c_{ijkl}(\mathbf{x})\varepsilon_{kl}(\mathbf{x},\tau) - e_{kij}(\mathbf{x})E_k(\mathbf{x},\tau) - d_{kij}(\mathbf{x})H_k(\mathbf{x},\tau) \tag{6}$$

$$D_j(\mathbf{x},\tau) = e_{jkl}(\mathbf{x})\varepsilon_{kl}(\mathbf{x},\tau) + h_{jk}(\mathbf{x})E_k(\mathbf{x},\tau) + \alpha_{jk}(\mathbf{x})H_k(\mathbf{x},\tau) \tag{7}$$

$$B_j(\mathbf{x},\tau) = d_{jkl}(\mathbf{x})\varepsilon_{kl}(\mathbf{x},\tau) + \alpha_{kj}(\mathbf{x})E_k(\mathbf{x},\tau) + \gamma_{jk}(\mathbf{x})H_k(\mathbf{x},\tau) \tag{8}$$

with the strain tensor ε_{ij} being related to the displacements u_i by

$$\varepsilon_{ij} = \frac{1}{2}\left(u_{i,j} + u_{j,i}\right) \tag{9}$$

The functional coefficients $c_{ijkl}(\mathbf{x})$, $h_{jk}(\mathbf{x})$ and $\gamma_{jk}(\mathbf{x})$ are the elastic coefficients, dielectric permittivities, and magnetic permeabilities, respectively; $e_{kij}(\mathbf{x})$, $d_{kij}(\mathbf{x})$ and $\alpha_{jk}(\mathbf{x})$ are the piezoelectric, piezomagnetic, and magnetoelectric coefficients, respectively. In the case of some crystal symmetries, one can formulate also the plane-deformation problems (Parton & Kudryavtsev, 1988) If $\varepsilon_{22} = \varepsilon_{23} = \varepsilon_{12} = E_2 = H_2 = 0$, the constitutive equations (6)-(8) are reduced to the following forms

$$\begin{bmatrix}\sigma_{11}\\ \sigma_{33}\\ \sigma_{13}\end{bmatrix} = \begin{bmatrix}c_{11} & c_{13} & 0\\ c_{13} & c_{33} & 0\\ 0 & 0 & c_{44}\end{bmatrix}\begin{bmatrix}\varepsilon_{11}\\ \varepsilon_{33}\\ 2\varepsilon_{13}\end{bmatrix} - \begin{bmatrix}0 & e_{31}\\ 0 & e_{33}\\ e_{15} & 0\end{bmatrix}\begin{bmatrix}E_1\\ E_3\end{bmatrix} - \begin{bmatrix}0 & d_{31}\\ 0 & d_{33}\\ d_{15} & 0\end{bmatrix}\begin{bmatrix}H_1\\ H_3\end{bmatrix} =$$

$$= \mathbf{C}(\mathbf{x})\begin{bmatrix}\varepsilon_{11}\\ \varepsilon_{33}\\ 2\varepsilon_{13}\end{bmatrix} - \mathbf{L}(\mathbf{x})\begin{bmatrix}E_1\\ E_3\end{bmatrix} - \mathbf{K}(\mathbf{x})\begin{bmatrix}H_1\\ H_3\end{bmatrix} \tag{10}$$

$$\begin{bmatrix}D_1\\ D_3\end{bmatrix} = \begin{bmatrix}0 & 0 & e_{15}\\ e_{31} & e_{33} & 0\end{bmatrix}\begin{bmatrix}\varepsilon_{11}\\ \varepsilon_{33}\\ 2\varepsilon_{13}\end{bmatrix} + \begin{bmatrix}h_{11} & 0\\ 0 & h_{33}\end{bmatrix}\begin{bmatrix}E_1\\ E_3\end{bmatrix} + \begin{bmatrix}\alpha_{11} & 0\\ 0 & \alpha_{33}\end{bmatrix}\begin{bmatrix}H_1\\ H_3\end{bmatrix} =$$

$$= \mathbf{G}(\mathbf{x})\begin{bmatrix}\varepsilon_{11}\\ \varepsilon_{33}\\ 2\varepsilon_{13}\end{bmatrix} + \mathbf{H}(\mathbf{x})\begin{bmatrix}E_1\\ E_3\end{bmatrix} + \mathbf{A}(\mathbf{x})\begin{bmatrix}H_1\\ H_3\end{bmatrix} \tag{11}$$

$$\begin{bmatrix} B_1 \\ B_3 \end{bmatrix} = \begin{bmatrix} 0 & 0 & d_{15} \\ d_{31} & d_{33} & 0 \end{bmatrix} \begin{bmatrix} \varepsilon_{11} \\ \varepsilon_{33} \\ 2\varepsilon_{13} \end{bmatrix} + \begin{bmatrix} \alpha_{11} & 0 \\ 0 & \alpha_{33} \end{bmatrix} \begin{bmatrix} E_1 \\ E_3 \end{bmatrix} + \begin{bmatrix} \gamma_{11} & 0 \\ 0 & \gamma_{33} \end{bmatrix} \begin{bmatrix} H_1 \\ H_3 \end{bmatrix} =$$

$$= \mathbf{R}(\mathbf{x}) \begin{bmatrix} \varepsilon_{11} \\ \varepsilon_{33} \\ 2\varepsilon_{13} \end{bmatrix} + \mathbf{A}(\mathbf{x}) \begin{bmatrix} E_1 \\ E_3 \end{bmatrix} + \mathbf{M}(\mathbf{x}) \begin{bmatrix} H_1 \\ H_3 \end{bmatrix} \qquad (12)$$

Instead of writing the global weak-form for the above governing equations, the MLPG method constructs a weak-form over the local fictitious subdomains such as Ω_s, which is a small region constructed for each node inside the global domain (Atluri, 2004). The local subdomains could be of any geometrical shape and size. In the present paper, the local subdomains are taken to be of a circular shape for simplicity. The local weak-form of the governing equation (5) can be written as (Sladek et al., 2008)

$$\int_{\Omega_s} \left[\sigma_{ij,j}(\mathbf{x},\tau) - \rho \ddot{u}_i(\mathbf{x},\tau) + X_i(\mathbf{x},\tau) \right] u_{ik}^*(\mathbf{x})\, d\Omega = 0 \qquad (13)$$

where $u_{ik}^*(\mathbf{x})$ is a test function.

Applying the Gauss divergence theorem to the first integral and choosing a Heaviside step function as the test function $u_{ik}^*(\mathbf{x})$ in each subdomain

$$u_{ik}^*(\mathbf{x}) = \begin{cases} \delta_{ik} & \text{at} \quad \mathbf{x} \in \Omega_s \\ 0 & \text{at} \quad \mathbf{x} \notin \Omega_s \end{cases},$$

One obtains the local boundary-domain integral equations

$$\int_{L_s+\Gamma_{su}} t_i(\mathbf{x},\tau) d\Gamma - \int_{\Omega_s} \rho \ddot{u}_i(\mathbf{x},\tau) d\Omega = - \int_{\Gamma_{st}} \tilde{t}_i(\mathbf{x},\tau) d\Gamma - \int_{\Omega_s} X_i(\mathbf{x},\tau) d\Omega \qquad (14)$$

where $\partial\Omega_s$ is the boundary of the local subdomain which consists of three parts $\partial\Omega_s = L_s \cup \Gamma_{st} \cup \Gamma_{su}$ (Sladek et al., 2008). Here, L_s is the local boundary that is totally inside the global domain, Γ_{st} is the part of the local boundary which coincides with the global traction boundary, i.e., $\Gamma_{st} = \partial\Omega_s \cap \Gamma_t$, and similarly Γ_{su} is the part of the local boundary that coincides with the global displacement boundary, i.e., $\Gamma_{su} = \partial\Omega_s \cap \Gamma_u$.

Nonhomogeneous material properties are included in eq. (14) through the elastic, piezoelectric and piezomagnetic coefficients involved in the traction components

$$t_i(\mathbf{x},\tau) = \left[c_{ijkl}(\mathbf{x}) u_{k,l}(\mathbf{x},\tau) + e_{kij}(\mathbf{x}) \psi_{,k}(\mathbf{x},\tau) + d_{kij}(\mathbf{x}) \mu_{,k}(\mathbf{x},\tau) \right] n_j(\mathbf{x})$$

Similarly, the local weak-form of the governing equation (1) can be written as

$$\int_{\Omega_s} \left[D_{j,j}(\mathbf{x},\tau) - R(\mathbf{x},\tau) \right] v^*(\mathbf{x})\, d\Omega = 0 \qquad (15)$$

where $v^*(\mathbf{x})$ is a test function.

Applying the Gauss divergence theorem to the local weak-form (15) and choosing the Heaviside step function as the test function $v^*(\mathbf{x})$, one can obtain

$$\int_{L_s+\Gamma_{sp}} Q(\mathbf{x},\tau) d\Gamma = - \int_{\Gamma_{sq}} \tilde{Q}(\mathbf{x},\tau) d\Gamma + \int_{\Omega_s} R(\mathbf{x},\tau) d\Omega \qquad (16)$$

where

$$Q(\mathbf{x},\tau) = D_j(\mathbf{x},\tau) n_j(\mathbf{x}) = \left[e_{jkl} u_{k,l}(\mathbf{x},\tau) - h_{jk} \psi_{,k}(\mathbf{x},\tau) - \alpha_{jk} \mu_{,k}(\mathbf{x},\tau) \right] n_j$$

The local integral equation corresponding to the governing equation (2) has the form

$$\int_{L_s+\Gamma_{sa}} S(\mathbf{x},\tau) d\Gamma = - \int_{\Gamma_{sb}} \tilde{S}(\mathbf{x},\tau) d\Gamma + \int_{\Omega_s} O(\mathbf{x},\tau) d\Omega, \qquad (17)$$

where the magnetic flux (normal component of the magnetic induction vector) is given by

$$S(\mathbf{x},\tau) = B_j(\mathbf{x},\tau) n_j(\mathbf{x}) = \left[d_{jkl} u_{k,l}(\mathbf{x},\tau) - \alpha_{kj} \psi_{,k}(\mathbf{x},\tau) - \gamma_{jk} \mu_{,k}(\mathbf{x},\tau) \right] n_j$$

The trial functions are chosen to be the MLS approximations by using a number of nodes spreading over the domain of influence. The approximated functions for the mechanical displacements, the electric and magnetic potentials can be written as (Belytschko et a., 1996)

$$\mathbf{u}^h(\mathbf{x},\tau) = \mathbf{\Phi}^T(\mathbf{x}) \cdot \hat{\mathbf{u}} = \sum_{a=1}^{n} \phi^a(\mathbf{x}) \hat{\mathbf{u}}^a(\tau),$$

$$\psi^h(\mathbf{x},\tau) = \sum_{a=1}^{n} \phi^a(\mathbf{x}) \hat{\psi}^a(\tau),$$

$$\mu^h(\mathbf{x},\tau) = \sum_{a=1}^{n} \phi^a(\mathbf{x}) \hat{\mu}^a(\tau), \qquad (18)$$

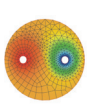

where the nodal values $\hat{\mathbf{u}}^a(\tau)=\left(\hat{u}_1^a(\tau),\,\hat{u}_3^a(\tau)\right)^T$, $\hat{\psi}^a(\tau)$ and $\hat{\mu}^a(\tau)$ are fictitious parameters for the displacements, the electric and magnetic potentials, respectively, and $\phi^a(\mathbf{x})$ is the shape function associated with the node a. The number of nodes n used for the approximation is determined by the weight functions $w^a(\mathbf{x})$. A 4th order spline-type weight function is applied in the present work

$$w^a(\mathbf{x})=\begin{cases}1-6\left(\dfrac{d^a}{r^a}\right)^2+8\left(\dfrac{d^a}{r^a}\right)^3-3\left(\dfrac{d^a}{r^a}\right)^4, & 0\le d^a\le r^a\\ 0, & d^a\ge r^a\end{cases} \tag{19}$$

where $d^a=\left\|\mathbf{x}-\mathbf{x}^a\right\|$ and r^a is the size of the support domain.

Then, the traction vector $t_i(\mathbf{x},\tau)$ at a boundary point $\mathbf{x}\in\partial\Omega_s$ is approximated in terms of the same nodal values $\hat{\mathbf{u}}^a(\tau)$ as

$$\mathbf{t}^h(\mathbf{x},\tau)=\mathbf{N}(\mathbf{x})\mathbf{C}(\mathbf{x})\sum_{a=1}^{n}\mathbf{B}^a(\mathbf{x})\hat{\mathbf{u}}^a(\tau)\;+$$
$$\mathbf{N}(\mathbf{x})\mathbf{L}(\mathbf{x})\sum_{a=1}^{n}\mathbf{P}^a(\mathbf{x})\hat{\psi}^a(\tau)+\mathbf{N}(\mathbf{x})\mathbf{K}(\mathbf{x})\sum_{a=1}^{n}\mathbf{P}^a(\mathbf{x})\hat{\mu}^a(\tau) \tag{20}$$

where the matrices $\mathbf{C}(\mathbf{x})$, $\mathbf{L}(\mathbf{x})$ and $\mathbf{K}(\mathbf{x})$ are defined in eq. (10), the matrix $\mathbf{N}(\mathbf{x})$ is related to the normal vector $\mathbf{n}(\mathbf{x})$ on $\partial\Omega_s$ by

$$\mathbf{N}(\mathbf{x})=\begin{bmatrix}n_1 & 0 & n_3\\ 0 & n_3 & n_1\end{bmatrix},$$

and finally, the matrices $\mathbf{B}^a$ and $\mathbf{P}^a$ are represented by the gradients of the shape functions as

$$\mathbf{B}^a(\mathbf{x})=\begin{bmatrix}\phi^a_{,1} & 0\\ 0 & \phi^a_{,3}\\ \phi^a_{,3} & \phi^a_{,1}\end{bmatrix},\quad \mathbf{P}^a(\mathbf{x})=\begin{bmatrix}\phi^a_{,1}\\ \phi^a_{,3}\end{bmatrix}$$

Similarly the normal component of the electric displacement vector $Q(\mathbf{x},\tau)$ can be approximated by

$$Q^h(\mathbf{x},\tau)=\mathbf{N}_1(\mathbf{x})\mathbf{G}(\mathbf{x})\sum_{a=1}^{n}\mathbf{B}^a(\mathbf{x})\hat{\mathbf{u}}^a(\tau)-$$
$$\mathbf{N}_1(\mathbf{x})\mathbf{H}(\mathbf{x})\sum_{a=1}^{n}\mathbf{P}^a(\mathbf{x})\hat{\psi}^a(\tau)-$$
$$\mathbf{N}_1(\mathbf{x})\mathbf{A}(\mathbf{x})\sum_{a=1}^{n}\mathbf{P}^a(\mathbf{x})\hat{\mu}^a(\tau) \tag{21}$$

where the matrices $\mathbf{G}(\mathbf{x})$, $\mathbf{H}(\mathbf{x})$ and $\mathbf{A}(\mathbf{x})$ are defined in eq. (11) and

$$\mathbf{N}_1(\mathbf{x})=\begin{bmatrix}n_1 & n_3\end{bmatrix}.$$

Eventually, the magnetic flux $S(\mathbf{x},\tau)$ is approximated by

$$S^h(\mathbf{x},\tau)=\mathbf{N}_1(\mathbf{x})\mathbf{R}(\mathbf{x})\sum_{a=1}^{n}\mathbf{B}^a(\mathbf{x})\hat{\mathbf{u}}^a(\tau)-$$
$$\mathbf{N}_1(\mathbf{x})\mathbf{A}(\mathbf{x})\sum_{a=1}^{n}\mathbf{P}^a(\mathbf{x})\hat{\psi}^a(\tau)-$$
$$\mathbf{N}_1(\mathbf{x})\mathbf{M}(\mathbf{x})\sum_{a=1}^{n}\mathbf{P}^a(\mathbf{x})\hat{\mu}^a(\tau) \tag{22}$$

with the matrices $\mathbf{R}(\mathbf{x})$, $\mathbf{A}(\mathbf{x})$ and $\mathbf{M}(\mathbf{x})$ being defined in eq. (12).

Furthermore, in view of the MLS-approximations (20)-(22) for the unknown quantities in the local boundary-domain integral equations (14), (16) and (17), we obtain their discretized forms as

$$\sum_{a=1}^{n}\left[\left(\int_{L_s+\Gamma_{st}}\mathbf{N}(\mathbf{x})\mathbf{C}(\mathbf{x})\mathbf{B}^a(\mathbf{x})d\Gamma\right)\hat{\mathbf{u}}^a(\tau)-\left(\int_{\Omega_s}\rho(\mathbf{x})\phi^a d\Omega\right)\ddot{\hat{\mathbf{u}}}^a(\tau)\right]+$$
$$\sum_{a=1}^{n}\left(\int_{L_s+\Gamma_{st}}\mathbf{N}(\mathbf{x})\mathbf{L}(\mathbf{x})\mathbf{P}^a(\mathbf{x})d\Gamma\right)\hat{\boldsymbol{\psi}}^a(\tau)\;+$$
$$\sum_{a=1}^{n}\left(\int_{L_s+\Gamma_{st}}\mathbf{N}(\mathbf{x})\mathbf{K}(\mathbf{x})\mathbf{P}^a(\mathbf{x})d\Gamma\right)\hat{\boldsymbol{\mu}}^a(\tau)=$$
$$=-\int_{\Gamma_{st}}\tilde{\mathbf{t}}(\mathbf{x},\tau)d\Gamma-\int_{\Omega_s}\mathbf{X}(\mathbf{x},\tau)d\Omega, \tag{23}$$

$$\sum_{a=1}^{n}\left(\int_{L_s+\Gamma_{sq}} \mathbf{N}_1(\mathbf{x})\mathbf{G}(\mathbf{x})\mathbf{B}^a(\mathbf{x})d\Gamma\right)\hat{\mathbf{u}}^a(\tau) \; - \sum_{a=1}^{n}\left(\int_{L_s+\Gamma_{sq}} \mathbf{N}_1(\mathbf{x})\mathbf{H}(\mathbf{x})\mathbf{P}^a(\mathbf{x})d\Gamma\right)\hat{\boldsymbol{\psi}}^a(\tau) - \sum_{a=1}^{n}\left(\int_{L_s+\Gamma_{sq}} \mathbf{N}_1(\mathbf{x})\mathbf{A}(\mathbf{x})\mathbf{P}^a(\mathbf{x})d\Gamma\right)\hat{\boldsymbol{\mu}}^a(\tau) = -\int_{\Gamma_{sq}} \tilde{Q}(\mathbf{x},\tau)d\Gamma + \int_{\Omega_s} R(\mathbf{x},\tau)d\Omega \qquad (24)$$

$$\sum_{a=1}^{n}\left(\int_{L_s+\Gamma_{sb}} \mathbf{N}_1(\mathbf{x})\mathbf{R}(\mathbf{x})\mathbf{B}^a(\mathbf{x})d\Gamma\right)\hat{\mathbf{u}}^a(\tau) \; - \sum_{a=1}^{n}\left(\int_{L_s+\Gamma_{sb}} \mathbf{N}_1(\mathbf{x})\mathbf{A}(\mathbf{x})\mathbf{P}^a(\mathbf{x})d\Gamma\right)\hat{\boldsymbol{\psi}}^a(\tau) - \sum_{a=1}^{n}\left(\int_{L_s+\Gamma_{sb}} \mathbf{N}_1(\mathbf{x})\mathbf{M}(\mathbf{x})\mathbf{P}^a(\mathbf{x})d\Gamma\right)\hat{\boldsymbol{\mu}}^a(\tau) = -\int_{\Gamma_{sb}} \tilde{S}(\mathbf{x},\tau)d\Gamma + \int_{\Omega_s} O(\mathbf{x},\tau)d\Omega \qquad (25)$$

which are considered on the subdomains adjacent to the interior nodes as well as to the boundary nodes on Γ_{st}, Γ_{sq} and Γ_{sb}. The essential boundary conditions on the global boundary are satisfied by collocating the approximation formulae (19).

The complete system of ordinary differential equations (23)-(25) can be rearranged in such a way that all known quantities are on the r.h.s. Thus, in matrix form the system becomes

$$\mathbf{F}\ddot{\mathbf{x}} + \mathbf{\Pi}\mathbf{x} = \mathbf{Y} \qquad (26)$$

The Houbolt method is applied, where the "acceleration" $\ddot{\mathbf{x}}$ is approximated by

$$\ddot{\mathbf{x}}_{\tau+\Delta\tau} = \frac{2\mathbf{x}_{\tau+\Delta\tau} - 5\mathbf{x}_{\tau} + 4\mathbf{x}_{\tau-\Delta\tau} - \mathbf{x}_{\tau-2\Delta\tau}}{\Delta\tau^2} \qquad (27)$$

where $\Delta\tau$ is the time-step.

Substituting eqs. (27) into eq. (26), we get the following system of linear algebraic equations for the unknowns $\mathbf{x}_{\tau+\Delta\tau}$

$$\left[\frac{2}{\Delta\tau^2}\mathbf{F} + \mathbf{\Pi}\right]\mathbf{x}_{\tau+\Delta\tau} = \frac{1}{\Delta\tau^2}5\mathbf{F}\mathbf{x}_{\tau} + \mathbf{F}\frac{1}{\Delta\tau^2}\left\{-4\mathbf{x}_{\tau-\Delta\tau} + \mathbf{x}_{\tau-2\Delta\tau}\right\} + \mathbf{Y} \qquad (28)$$

3. NUMERICAL EXAMPLES

An edge crack in a finite magnetoelectroelastic strip is analyzed. The following geometrical parameters are considered: crack length, $a = 0.5$, $a/w = 0.4$ and $h/w = 1.2$, where w is the specimen width and h is the specimen height. Due to the symmetry of the problem with respect to the x_1-axis, only a half of the strip is modeled. We have used 930 equidistantly distributed nodes for the MLS approximation of the physical fields. The top of the strip is subjected to an impact mechanical load with the Heaviside time variation and the amplitude $\sigma_0 = 1$ Pa. An exponential variation of the elastic, piezoelectric, dielectric, paramagnetic, electromagnetic and magnetic permeability coefficients are assumed as

$$f_{ij}(\mathbf{x}) = f_{ij0}\exp(\gamma_f x_1), \qquad (29)$$

where f_{ij0} corresponds to the $BaTiO_3$-$CoFe_2O_4$.

For simplicity, we have used the same gradient parameters for all material coefficients with the value $\gamma = 2$ in the numerical calculations. The impermeable crack-face boundary conditions for the electrical and magnetic fields are considered. The time variation of the normalized mode-I stress intensity factor (SIF) is given in figure 1, where $K_I^{stat} = 2.64\text{Pa}\cdot\text{m}^{1/2}$. Recall that the elastic wave velocities are increasing with x_1, since the mechanical parameters of FGMs are increasing in the x_1-direction and the mass density is uniform. Therefore, the peak values of the mode-I SIF are reached at a shorter time instant in functionally graded strip than in a homogeneous one.

The time variations of the electric displacement intensity factor (EDIF) and magnetic induction intensity factor (MIIF) are given in figures 2 and 3. The intensity factors for crack problems in magnetoelectroelastic solids are evaluated from the conservation integral representations for the SIFs, EDIF and MIIF which have been recently derived by authors. Again the peak values of the EDIF and MIIF are shifted to shorter time instants in the FGM strip than in a homogeneous one. All three peaks for the SIF, EDIF and MIIF factors are reached almost at the same time instants.

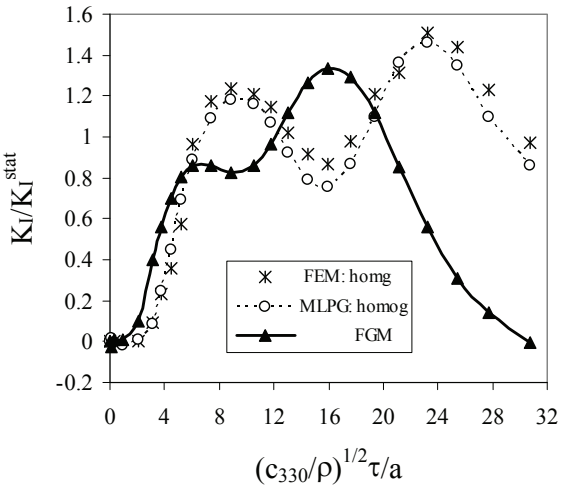

Fig. 1. *Normalized mode-I SIF for an edge crack in a strip under a pure mechanical load.*

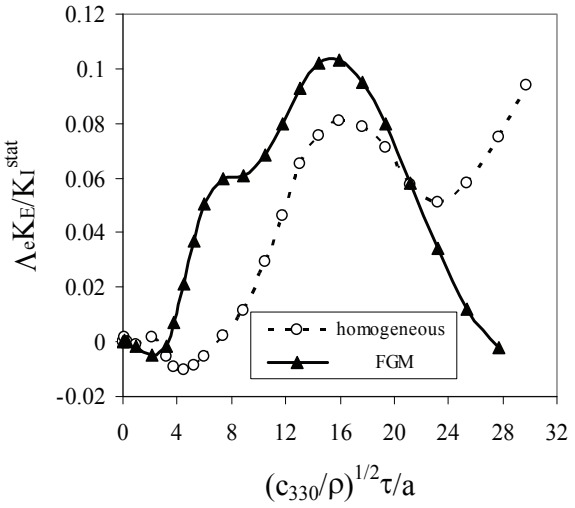

Fig. 2. *Normalized EDIF for an edge crack in a strip under a pure mechanical load.*

For normalized electrical displacement and magnetic induction intensity factors we have used the normalization parameters $\Lambda_e = e_{33}/h_{33}$ and $\Lambda_m = d_{33}/\gamma_{33}$, respectively.

4. CONCLUSIONS

A meshless local Petrov-Galerkin method (MLPG) is applied for 2-D crack problems in continuously nonhomogeneous magnetoelectroelastic solids subjected to a mechanical loading. The inertial term is considered in the equations of motion. The coupled governing partial differential equations are satisfied in a weak-form on small fictitious subdomains. A unit step function is used as the test function in the local weak-form of the governing partial differential equations on small circular subdomains spread on the analyzed domain. The moving least-squares (MLS) scheme is adopted for the approximation of the physical field quantities. One obtains a system of ordinary differential equations for certain nodal unknowns. That system is solved numerically by the Houbolt finite-difference scheme. The proposed method is a truly meshless method, which requires neither domain elements nor background cells in either the interpolation or the integration.

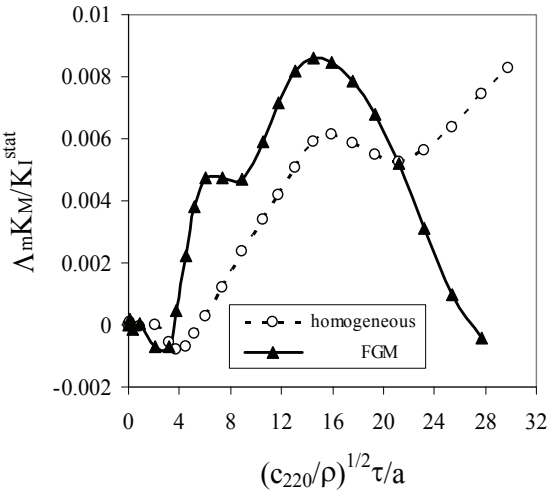

Fig. 3. *Normalized MIIF for an edge crack in a strip under a pure mechanical load.*

ACKNOWLEDGEMENTS

The authors acknowledge the support by the Slovak Science and Technology Assistance Agency registered under number APVV-0427-07, the Slovak Grant Agency VEGA-2/0039/09.

REFERENCES

Atluri, S.N., 2004, *The Meshless Method, (MLPG) for Domain & BIE Discretizations*, Tech Science Press, Forsyth.

Belytschko, T., Krogauz, Y., Organ, D., Fleming, M., Krysl, P., 1996, Meshless methods; an overview and recent developments, *Comp. Meth. Appl. Mech. Engn.*, 139, 3-47.

Liu G.R., Dai K.Y., Lim K.M., Gu Y.T., A point interpolation mesh free method for static and frequency analysis of two-dimensional piezoelectric structures, Computational Mechanics, 29, 2002, 510-519.

Ohs, R.R., Aluru, N.R., 2001, Meshless analysis of piezoelectric devices, *Computational Mechanics*, 27, 23-36.

Parton, V.Z., Kudryavtsev, B.A.,1988, *Electromagnetoelasticity, Piezoelectrics and Electrically Conductive Solids*, Gordon and Breach Science Publishers, New York.

Sladek, J., Sladek, V., Zhang, Ch., Solek, P., 2007, Application of the MLPG to thermo-piezoelectricity, *CMES: Computer Modeling in Engineering & Sciences*, 22, 217-233.

Sladek, J., Sladek, V., Solek, P., Pan, E., 2008, Fracture analysis of cracks in magneto-electro-elastic solids by the MLPG, *Computational Mechanics,* 42, 697-714.

Tong, Z.H., Lo, S.H., Jiang, C.P., Cheung, Y.K., 2008, An exact solution for the three-phase thermo-electro-magneto-elastic cylinder model and its application to piezoelectric-magnetic fiber composites, *Int. J. Solids and Structures*, 45, 5205-5219.

ANALIZA METODĄ MLPG PROBLEMÓW PĘKANIA W CIAŁACH MAGNETOELEKTRYCZNYCH

Streszczenie

Bezsiatkowa metoda oparta na lokalnym schemacie Petrova-Galerkina została zastosowana do rozwiązania zadania brzegowego powstawania pęknięć w ciałach magnetoelektrycznych. Testy wykonano dla jednostkowej funkcji skokowej w lokalnie słabym sformułowaniu. Prowadzi to do lokalnych brzegowych równań całkowych (ang. local boundary-domain integral equations – (LIEs). Przesuwna metoda najmniejszych kwadratów (ang. moving least-squares – MLS) została zaadoptowana do aproksymacji wielkości fizycznych w LIEs. Otrzymano układ zwyczajnych równań różniczkowych dla pewnych zmiennych węzłowych. Układ równań jest rozwiązywany metodą różnic skończonych stosując schemat Houbolta. Wyniki numerycznych obliczeń wskaźników intensywności w materiałach jednorodnych oraz w materiałach z gradientem własności są przedstawione w pracy.

Received: September 9, 2010
Received in a revised form: October 17, 2010
Accepted: November 24, 2010